Temperature-Induced Nanostructure Formation Behavior of Core Cross-Linked Star-Shaped Poly(*N*-isopropylacrylamide) in water

Ken Terao,[*,†] *Masahiro Abe,*[†] *Masafumi Nagase,*[†] *Sayuri Takeshima,*[‡] *Shohei Ida,*[‡] *and Shokyoku Kanaoka*[*,‡]

[†]Department of Macromolecular Science, Graduate School of Science, Osaka University, 1-1 Machikaneyama-cho, Toyonaka, Osaka 560-0043, Japan

[‡]Department of Materials Chemistry, Faculty of Engineering, The University of Shiga Prefecture, 2500 Hassaka, Hikone, Shiga 522-8533, Japan

* Corresponding author. E-mail address: terao.ken.sci@osaka-u.ac.jp

For Table of Contents Use Only

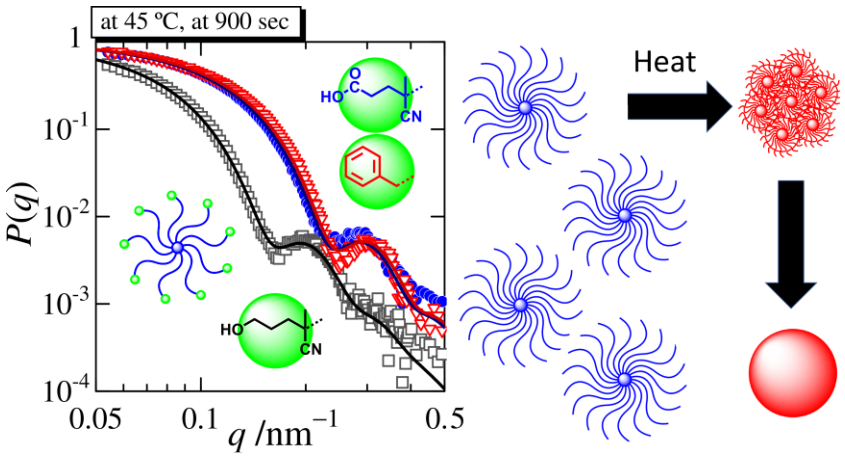

ABSTRACT

Small-angle X-ray scattering and electrophoretic light scattering measurements were made for dilute aqueous solutions of star-branched poly(*N*-isopropylacrylamide) (sPNIPAM) at different temperatures. In the constant heating process, relatively narrow-dispersed sphere particles with an average aggregation number between 10 and 50 were observed in water at high temperatures (45 – 55 °C) regardless of the end groups: carboxyl, hydroxyl, and benzyl groups. Indeed, the test solutions for which the polymer mass concentration was 2 – 4 mg mL^{-1} did not become turbid at temperatures higher than the phase separation temperature of the corresponding linear polymer. Negative ζ potential was found for all solutions at the high temperature, 45 °C, indicating that electrostatic repulsion force stabilizes the dispersion state. Spinodal decomposition is the dominant mechanism of the microscopic phase separation because narrower distributed spherical particles were observed in the solution upon rapid heating than that for the constant heating procedure.

Introduction

Poly(*N*-isopropylacrylamide) (PNIPAM) is one of the most well-investigated thermosensitive polymers[1] since the LCST-type phase separation behavior of aqueous solution was first reported by Heskins et al.[2] in 1968. The aqueous solution of PNIPAM, however, does not attain macroscopic liquid-liquid phase separation. The phase diagram was thus estimated from the cloud point temperature. The thermal history of the solution influences the dispersion behavior of the submicron-sized droplet consisting of a concentrated PNIPAM soluiton.[3] Size and number of molecules in each droplet generally thus depend on the polymer mass concentration c. Indeed, small globular nanoparticles consisting of a single PNIPAM chain can be observed for a very dilute regime at $c = 6.7 \times 10^{-7}$ g cm^{-3} at high temperatures,[4] and submicron-sized aggregates can be also observed for normal dilute solutions.[5-7]

Phase diagram of the PNIPAM-water system can be influenced even by a few branches.[8] Well-designed branched PNIPAM has thus been investigated, especially for star-branched PNIPAM (sPNIPAM). The cloud point temperature somewhat depends on the chemical structure of the end and branching points.[9-12] As in the case of linear PNIPAM, single molecular globules can be observed for a very dilute solution (c = 1 or 5×10^{-6} g cm^{-3}) of sPNIPAM when the hyperbranched polymer was chosen as the core.[13, 14] Recently, it was reported that the aqueous solution of sPNIPAM with carboxyl end groups kept high transparency even at 70 °C[15] and the aggregation number can be controlled by pH and temperature.[16] These results are much different from UCST-type phase separation behavior of nonpolar star polymers in poor solvents,[17-20] suggesting that sPNIPAM is a better source to evaluate nanometer-sized materials induced by the temperature change.

As a first step of this research, we observed specific scattering patterns for spherical nanoparticles with relatively narrow size distribution for sPNIPAM in water above the phase separation temperature of linear PNIPAM. To reveal the structural characteristics of the spherical particles in water at high temperatures, small-angle X-ray scattering (SAXS) measurements were carried out for sPNIPAM samples with different end groups in water at different temperatures and temperature changing rate. Electrophoretic light scattering measurement was also made for the solution to clarify the stability of the colloidal dispersion consisting of sPNIPAM in water.

Experimental Section

Samples. Three sPNIPAM samples reported in ref 15 were used for this study. Samples **S1** and **S2** are designated to be **s(PN96)35C** and **s(PN125)25O**, respectively. The chemical structure including the chain ends and the branching core is illustrated in Chart 1. The number-average degree of polymerization $DP_{n,arm}$ of the arm chain was determined by ^{1}H NMR spectra, and the dispersity index $Đ$ was estimated by GPC measurement with PMMA standard to be between 1.1 and 1.2 where $Đ$ is defined as the ratio of weight- to number-average molar masses. The weight-average molar mass $M_{w,star}$ of the star polymer was determined in terms of the SEC-MALS measurement. The arm number N_{arm} was calculated considering the composition of the branching core. Four more samples, **s(PN57)28C**, **s(PN50)35Bz**, **s(PN97)19Bz,** and **s(PN188)21Bz**, were synthesized and characterized in the same manner reported previously.[15] The values of $DP_{n,arm}$, $M_{w,star}$, and N_{arm} are summarized in Table 1. Note that the $Đ$ values for the star polymer samples were between 1.2 and 1.3.

Chart 1. Chemical Structure of sPNIPAM samples.

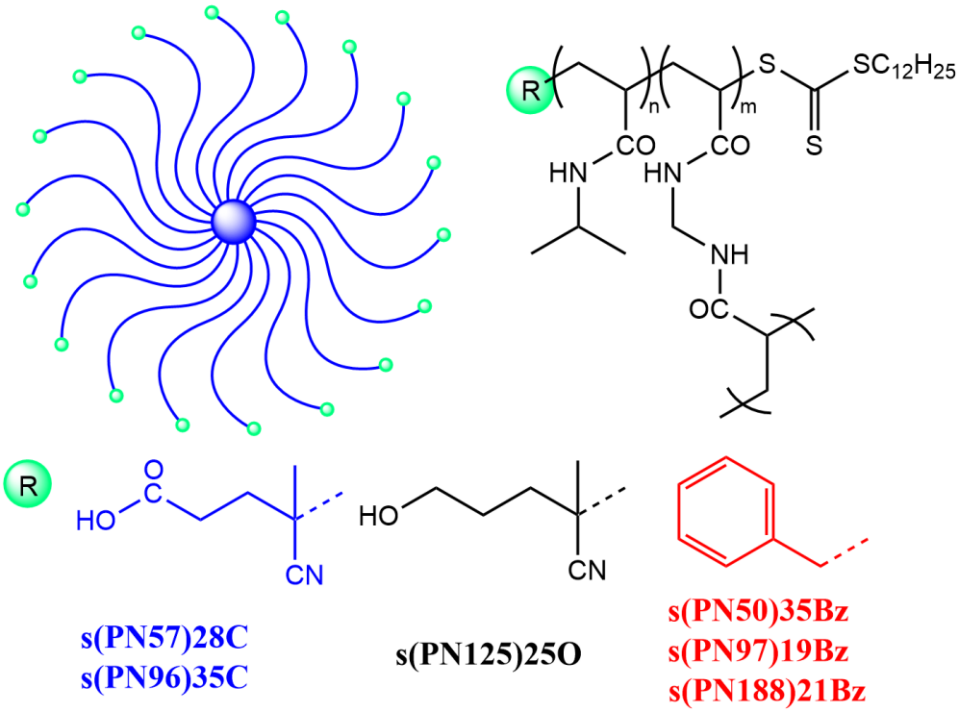

Table 1. Molecular Characteristics of sPNIPAM Samples

Samples	$DP_{n,arm}$ [a]	$M_{w,star}$ [b] /kg mol^{-1}	N_{arms}	ζ / mV 15 °C	ζ / mV 45 °C	Constant heating, At 55 °C			Rapid heating to 45 °C, kept 900 sec		
						N_{agg}	R_m/nm	σ_R	N_{agg}	R_m/ nm	σ_R
s(PN57)28C	57	263	28	−5.9	−28	10	19.0	0.14	6.9	17.2	0.12
s(PN96)35C [c]	96	510	35	−7.4	−22	8.8	17.0	0.19	10.8	19.3	0.12
s(PN125)25O [d]	125	460	25	0.3	−26	52	31.0	0.17	40.2	28.3	0.13
s(PN50)35Bz	50	289	35	−4.5	−42	–	26.0	0.21	–	28.0	0.25
s(PN97)19Bz	97	273	19	−5.3	−17	7.4	18.0	0.13	9.2	18.8	0.12
s(PN188)21Bz	188	582	21	−3.0	−24	16	25.5	0.16	12.5	26.0	0.14

[a] From ^{1}H NMR. [b] From SEC-MALS. [c] Sample **S1** in ref. 15. [d] Sample **S2** in ref. 15.

Electrophoretic Light Scattering (ELS) Measurement. The electrophoretic mobility u for the six sPNIPAM samples in pure water with the polymer mass concentration c being 2.0 mg mL^{-1} was measured by using an Otsuka zeta-potential analyzer ELSZ-2 both at 15 and 45 °C. The ζ potential was calculated from u by the Smoluchowski equation.

Small-angle X-ray Scattering (SAXS). Synchrotron radiation SAXS measurements were carried out for the six sPNIPAM samples in pure water and 20 mM aqueous NaCl at the BL40B2 beamline in SPring-8 (Hyogo, Japan). The wavelength λ_0 in a vacuum and the sample-to-detector distance l_{sd} were set to be 0.10 nm and 4.2 m, respectively. The scattered light was acquired with a Dectris Pilatus 3 2M photon-counting detector. Silver behenate was used as a calibrant to determine the beam center on the detector and l_{sd}. A capillary cell, in which a 2 mmϕ quartz capillary was fixed in a thin aluminum block, was installed into a HCS402 thermostatic cell holder (Instec). The scattered light intensity was normalized by the intensity of the incident light detected at the lower end of the cell to compensate for both the intensity of light source and solution transmittance. SAngler software[21] was utilized to evaluate the scattering intensity as a function of the magnitude q of the scattering vector. The excess scattering intensity $\Delta I(q)$ of the solutions was evaluated by subtracting the scattering intensity of the solvent in the same capillary cell. Two kinds of temperature change were tested for each solution. The first attempt is that the solution was gradually heated from 15 °C to 55 °C at a constant rate of 1 K min^{-1}. The second attempt is that the temperature of the solution was rapidly changed from 15 °C to 45 °C, and time-resolved SAXS measurement was examined for the solution; note that the cell and cell holder were the same as those used for the kinetic study of a double helical polysaccharide.[22] Integration time for each SAXS measurement was 60 s. The reduced scattering intensity R_q was estimated from $\Delta I(q)$

assuming molecular dispersion at 15 °C. In other words, R_q at $q = 0$ (R_0) has a relation of $R_0/Kc = M_{w,star}$ where K is the optical constant of the X-ray scattering.

Results and Discussion

Solubility in Water and ζ Potential. All six sPNIPAM samples are soluble in pure water and 20 mM aqueous NaCl at 15 °C. The aqueous solutions at c = 2 mg mL^{-1} were still transparent in water even at 55 °C, whereas the aqueous linear PNIPAM solution got turbid at about 40 °C even in a dilute regime. It is noted that the appreciable turbidity was observed for **s(PN97)19Bz** and **s(PN125)25O** at a higher concentration range (10 – 20 mg mL^{-1}) while the cloud point temperature was somewhat higher than the corresponding arm (linear) chain.[15] As shown in Table 1, appreciable large negative ζ potentials between −17 mV and −42 mV were observed at 45 °C irrespective of the end groups, while smaller absolute values of ζ were evaluated at 15 °C, suggesting the negative surface electric potential of the PNIPAM nanoparticles in water at 45 °C. Similar temperature-dependent electrophoretic behavior was also reported for neutral PNIPAM microgel particles.[23] They proposed that hydroxide ions adsorb on the hydrophobic interface of the PNIPAM particles above the phase separation temperature of PNIPAM in water. Furthermore, the obtained ζ potential at 45 °C is similar to that for colloidal silica,[24] suggesting that the high transparency of the solution at 45 °C is most likely due to the electrostatic repulsion between the formed nanoparticles. It is supported by that sPNIPAM solutions in 20 mM aqueous NaCl became turbid at 45 °C.

Nanoparticles Formation Behavior upon Constant Heating. Scattering profiles, double logarithmic plots of R_q/Kc vs q for six sPNIPAM samples at c = 2 mg mL^{-1} upon constant heating with the heating rate r_T of 1.0 K min^{-1} are illustrated in Figure 1. At 15 °C, mostly flat region is

found at the low q end except for panel d for **s(PN50)35Bz**. A monotonical decrease of R_q/Kc with increasing q at the temperature is typical for molecularly dispersed polymer chains in dilute solution. Extrapolation of R_q/Kc to $q = 0$ at all the temperatures investigated was examined with the Guinier plot as shown in Figure S1 in the supporting information to evaluate the radius of gyration R_g at all the temperatures and the aggregation number N_{agg} between 16 and 55 °C except for **s(PN50)35Bz** as described below. The N_{agg} values were evaluated as the ratio of R_0/Kc to that at 15 °C. Intermolecular interactions do not appreciably influence the extrapolated data because of substantially no concentration dependence in the scattering profiles at least for **s(PN57)28C** and **s(PN125)25O** at 15 °C as is shown in Figure S2. On the other hand, characteristic scattering profiles are found at 55 °C with a much higher scattering intensity at the low q end, suggesting the formation of spherical nanoparticles with relatively narrow size dispersity.

The evaluated N_{agg} and R_g data are plotted against temperature in Figure 2 in which we omitted the N_{agg} data for **s(PN50)35Bz** because the scattering intensity at $q = 0$ and at 18 °C was appreciably smaller than that at 15 °C, suggesting the aggregation even at the lowest temperature. Indeed, the R_g value for **s(PN50)35Bz** at 15 °C is much larger than those for **s(PN97)19Bz** and **s(PN188)21Bz**. The N_{agg} values for **s(PN57)28C**, **s(PN96)35C**, and **s(PN125)25O** increase gradually between 15 and 30 °C, rapidly raise between 30 and 35 °C, and reach each asymptotic value at higher temperatures. A similar sudden thermally induced change of N_{agg} above 30 °C is also found for **s(PN97)19Bz** and **s(PN188)21Bz** while the N_{agg} is almost independent of T between 15 and 30 °C, suggesting that the aggregation temperature is mostly free from the end groups. This is reasonable because the phase separation temperature of random copolymers of PNIPAM and acrylamide only gradually changed with increasing the composition of acrylacmide.[25] The N_{agg} values at the highest temperature are between 9 and 52, indicating that sPNIPAM samples form

spherical aggregates consisting of a relatively small number of polymer molecules. The resulting molar mass for **s(PN125)25O** at 55 °C is quite larger than that of the other star polymer samples except for **s(PN50)35Bz**. Not only the chemical structure of the chain end but also the side chain length, arm numbers, and weight fraction of the gel core can affect N_{agg}.

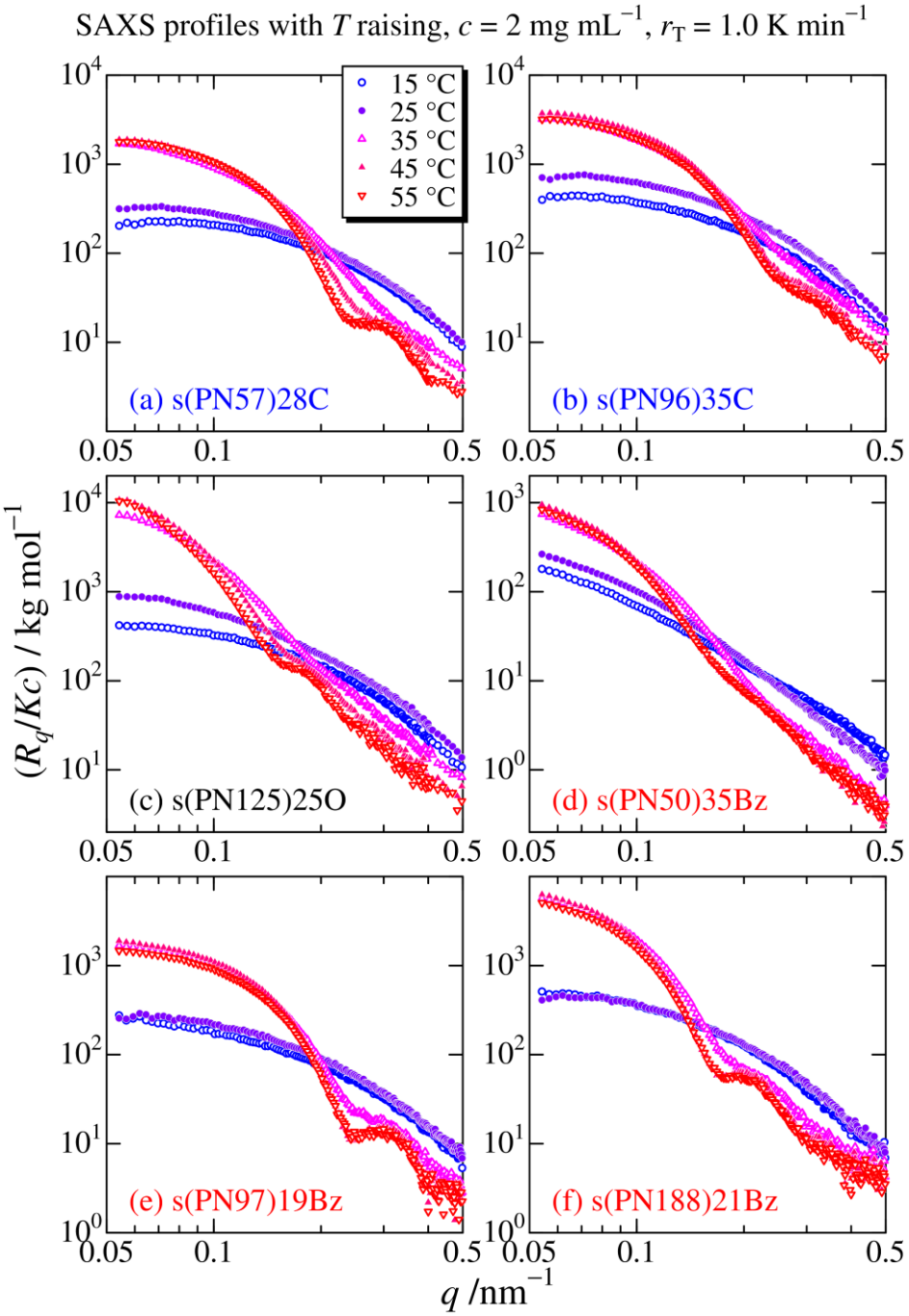

Figure 1. Magnitude q of the scattering vector dependence of the reduced scattering intensity R_q/Kc for the indicated sPNIPAM samples in water. The temperature was raised at the rate of r_T = 1.0 K min^{-1} and the polymer mass concentration was c = 2 mg mL^{-1}.

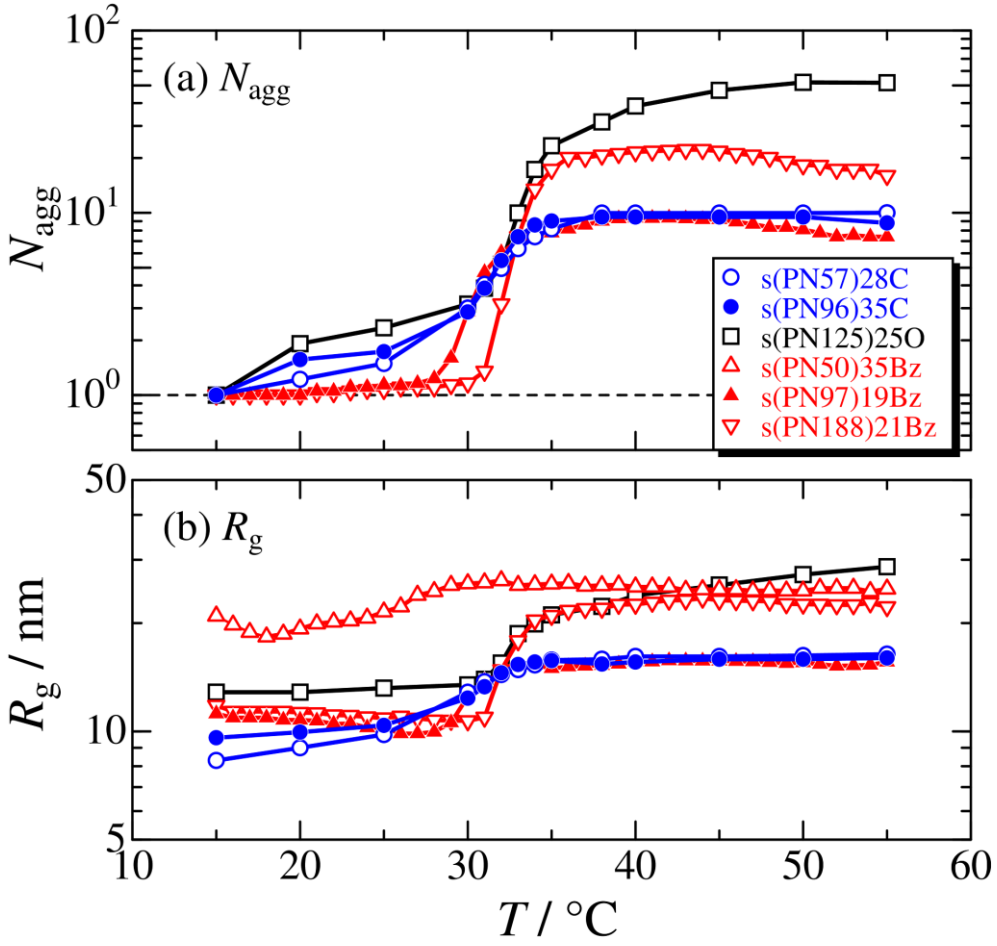

Figure 2. Temperature dependence of apparent aggregation number $N_{agg,app}$ and gyration radius $R_{g,app}$ for the indicated sPNIPAM samples in water. r_T = 1.0 K min^{-1} and c = 2 mg mL^{-1}.

The form factor $P(q)$ for each sample was evaluated from R_q / R_0 where R_0 was estimated from the Guinier plot (Figure S1). The resulting $P(q)$ data are plotted against q in Figure 3. We attempted to analyze the data in terms of the polydisperse sphere because the shape of $P(q)$ is substantially similar to colloidal silica.[26] Assuming log normal distribution of the diameter R, $P(q)$ for the polydisperse sphere is expressed as

$$P(q) = \frac{\int_0^\infty \Phi^2(qR) w(R) R^3 \mathrm{d}R}{\int_0^\infty w(R) R^3 \mathrm{d}R} \qquad (1)$$

with

$$\Phi(x) = \frac{3(\sin x - x\cos x)}{x^3} \quad (2)$$

$$w(R) = \frac{1}{\sqrt{2\pi}\sigma_R R}\exp\left\{-\frac{[\ln(R/R_m)]^2}{2{\sigma_R}^2}\right\} \quad (3)$$

where R_m and σ_R are the parameters of the radius dispersion. A curve-fitting procedure was employed to evaluate the most fitted theoretical curves in Figure 3. The resulting parameters are summarized in Table 1. The calculated *z*-average radius of gyration from R_m and σ_R is in agreement with the R_g value from the Guinier plot within ±3%. The σ_R values except for the **s(PN50)35Bz** range between 0.13 and 0.19, corresponding to the molar mass dispersity $Đ$ between 1.16 and 1.3. A somewhat larger σ_R for **s(PN50)35Bz** is most likely due to the less dispersibility even at low temperatures. In any case, sPNIPAM samples form nanometer-sized spherical particles with relatively narrow size distribution in pure water, regardless of the end groups. Assuming molecular dispersion at 15 °C except for **s(PN50)35Bz** and the uniform polymer concentration in the spherical particles, we may estimate the internal polymer mass concentration c_{in} of the particles as $c_{in} = 3M_{w,star}N_{agg}/4\pi R_m^3 N_A$. The resulting c_{in} values are between 0.14 and 0.36 g cm^{-3}. It should be noted that the calculated value may be slightly underestimated if there is a small amount of molecularly dispersed sPNIPAM molecules in the solution. In any case, these values are much smaller than those for the internal concentrations in the spherical droplet consisting of linear PNIPAM in water.[7]

As mentioned above, while high transparency of the solution is only observed for sPNIPAM-pure water systems, significant turbidity was observed for sPNIPAM in aqueous NaCl. This is also found in our SAXS data. Figure S3 in the supporting information shows double logarithmic plots of R_q/Kc vs q for **s(PN97)19Bz** in 20 mM aqueous NaCl. The scattering profile

at low temperatures at 15 and 25 °C are substantially the same as those in pure water as shown in Figure 1e but much weaker scattering intensities were observed at higher temperatures, indicating macroscopic phase separation. Indeed, we recognized the appreciable turbidity of the solution with the naked eye.

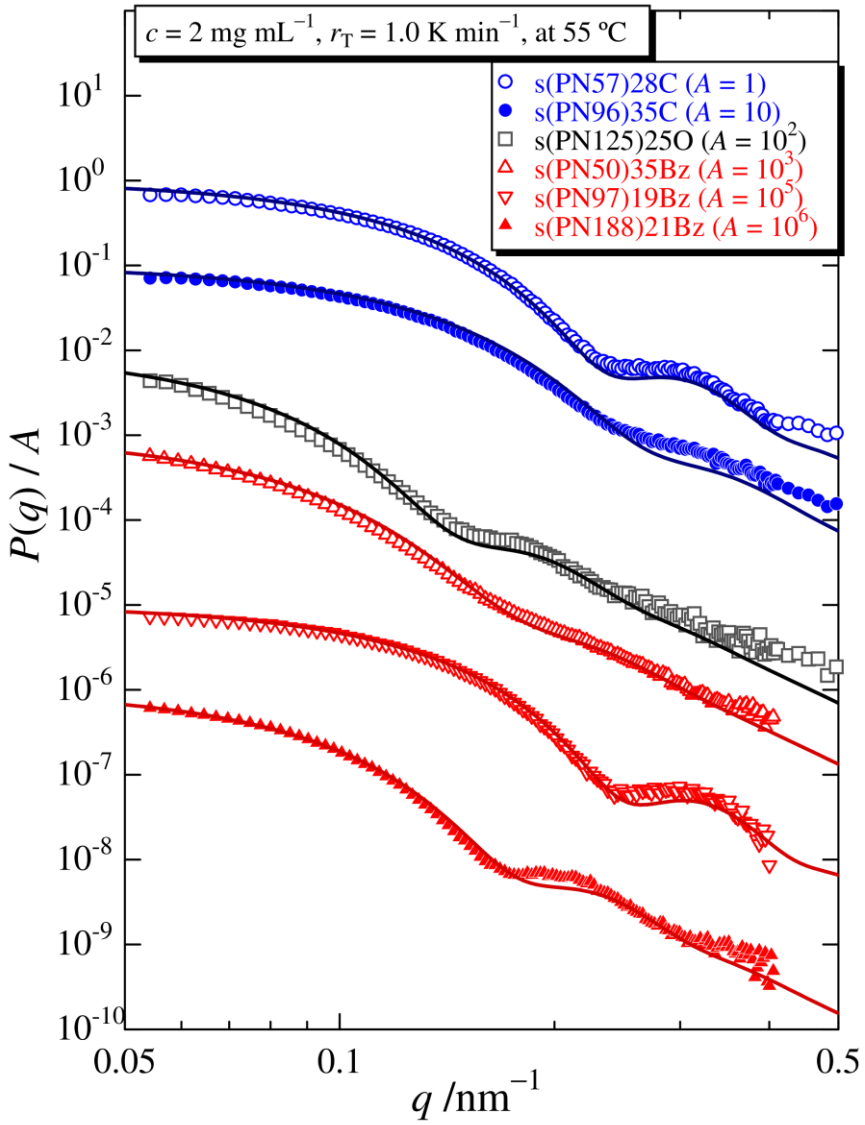

Figure 3. Double logarithmic plots of the form factor $P(q)$ vs q for the indicated sPNIPAM samples in water at 55 °C. r_T = 1.0 K min^{-1} and c = 2 mg mL^{-1}. Solid curves, theoretical values for eqs 1-3 with the parameters in Table 1.

Nanoparticle Formation Behavior upon Rapid Heating. In our preliminary SAXS experiments on a dilute solution of sPNIPAM samples, the appreciable time dependence of the scattering profiles was observed at high temperatures after rapid heating. We thus made time-resolved SAXS measurements after rapid heat treatment. Double logarithmic plots of R_q/Kc vs q at different times are shown in Figure 4 in which the reduced scattering intensity was calibrated by the R_q/Kc value at 15 °C. The time zero is defined as that the cell temperature became within ±0.2 °C of the target temperature, which is approximately one minute after starting the temperature change. The appreciable time dependence is only found for sPNIPAM samples with carboxyl end groups, **s(PN57)28C** and **s(PN96)35C**, suggesting that surface condition and/or viscoelastic properties of nanoparticles just after heating depends on the end groups. In any case, the scattering intensity became mostly time-independent after 600 s, indicating high dispersibility of the nanoparticles in pure water. The resulting nanoparticles have a similar surface taking into the similar ζ potential account. The Guinier plots were constructed for the R_q/Kc at 900 s to evaluate N_{agg} and R_g (Figure S4). The resulting N_{agg} values in Table 1 are not very different from those at 55 °C (and also 45 °C) with the constant heating treatment, indicating that the average molar mass of the resulting nanoparticles is not substantially influenced by r_T.

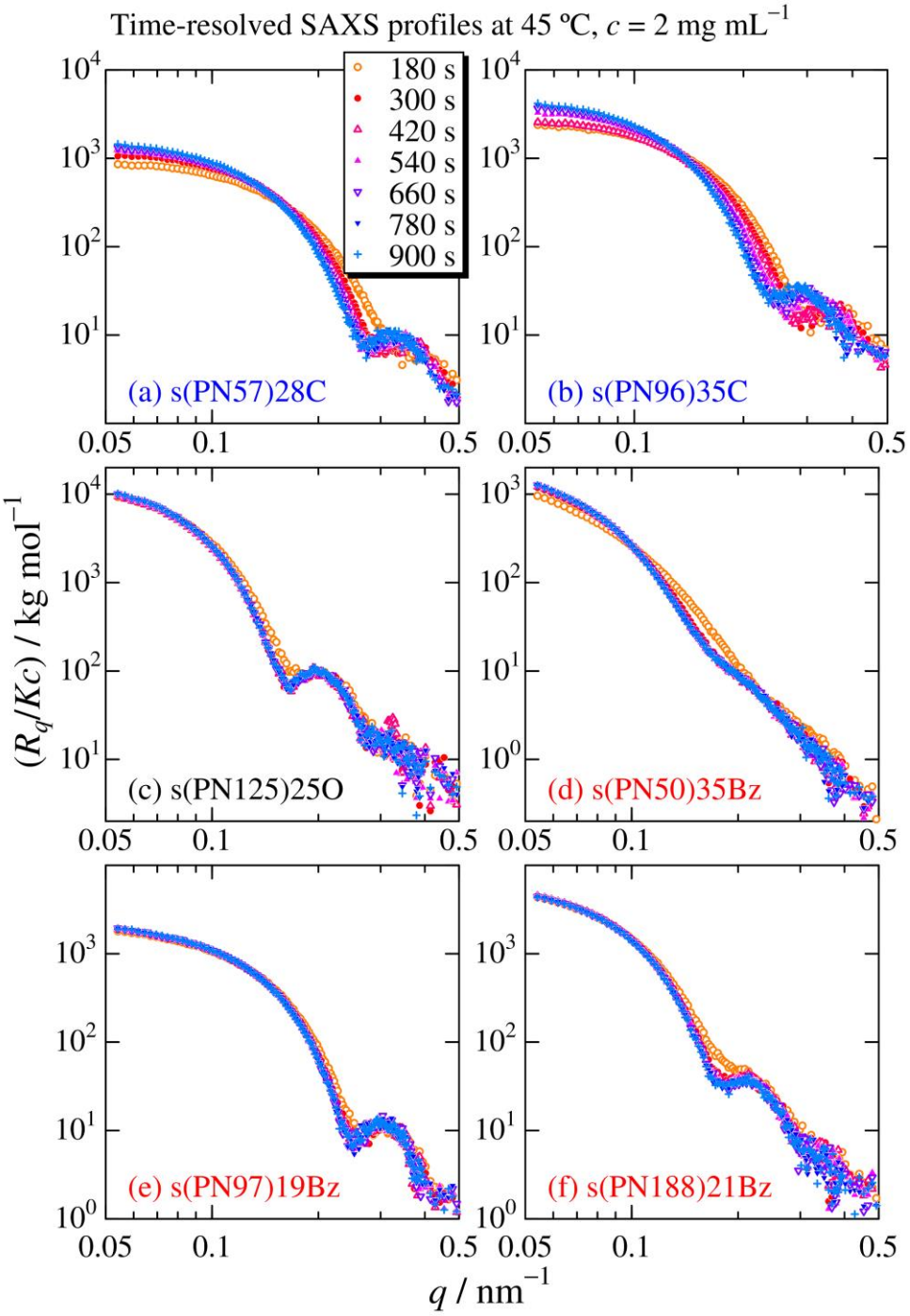

Figure 4. Results of the time-resolved SAXS experiments after rapid heat from 15 °C to 45 °C for the indicated sPNIPAM samples in water at c = 2 mg mL^{-1}. Symbols are the scattered R_q/Kc at the indicated time from the rapid heating.

The form factor $P(q)$ data at 900 s after rapid heating are double logarithmically plotted against q in Figure 5. Interestingly, scattering profiles at 900 s except for **s(PN50)35Bz** have typical shape for nanosized spheres with narrower size distribution than those in Figure 3. The experimental data were analyzed by eqs 1-3 to determine R_m and σ_R. z-Average radii of gyration calculated from the parameters were substantially the same within ±2% as those from the Guinier plots except for **s(PN50)35Bz**. The distribution parameter σ_R of 0.12 – 0.14 corresponds to $Đ$ of 1.14 – 1.19. The internal concentration c_{in} is calculated to be between 0.14 and 0.32 g cm^{-3}. This is substantially the same as those upon the constant heating process mentioned above. The smaller σ_R values indicate that more uniformly sized nanoparticles are generated via rapid heating than those for the constant heating. This is most likely because the spinodal decomposition was a dominant mechanism, especially in the rapid heating process. Micrometer-sized particle fabrication with the spinodal decomposition was also reported for the polystyrene-cyclohexane system with a glass bead core.[27]

We demonstrated that sPNIPAM can form uniform-sized nanosphere with increasing temperature. These phenomena were found for sPNIPAM samples with different end groups: carboxyl, hydroxyl, and benzyl, indicating that the star-branched structure plays a decisive role to form the nanoparticles. Much wider dispersion was, on the other hand, indicated for linear PNIPAM in water[7] though some dynamic light scattering data suggest narrow dispersity even for linear PNIPAM.[6] One of the possible reasons to form nanospheres with narrow distribution for the current star polymer is that much smaller dimensional properties of the star than those for the linear polymer with the same molar mass. Therefore, it takes a short time to form concentrated droplets from early aggregates compared with the linear PNIPAM as illustrated in Figure 6. It is thus expected that temperature-responsive polymers with high segment density in solution may

have similar phenomena. Indeed, nanoparticle formation behavior was reported for PNIPAM graft dextran in terms of dynamic light scattering and electron microscopy.[28] It is desirable to investigate nanoparticle formation behavior for the other star, comb, and hyperbranched polymers in solution.

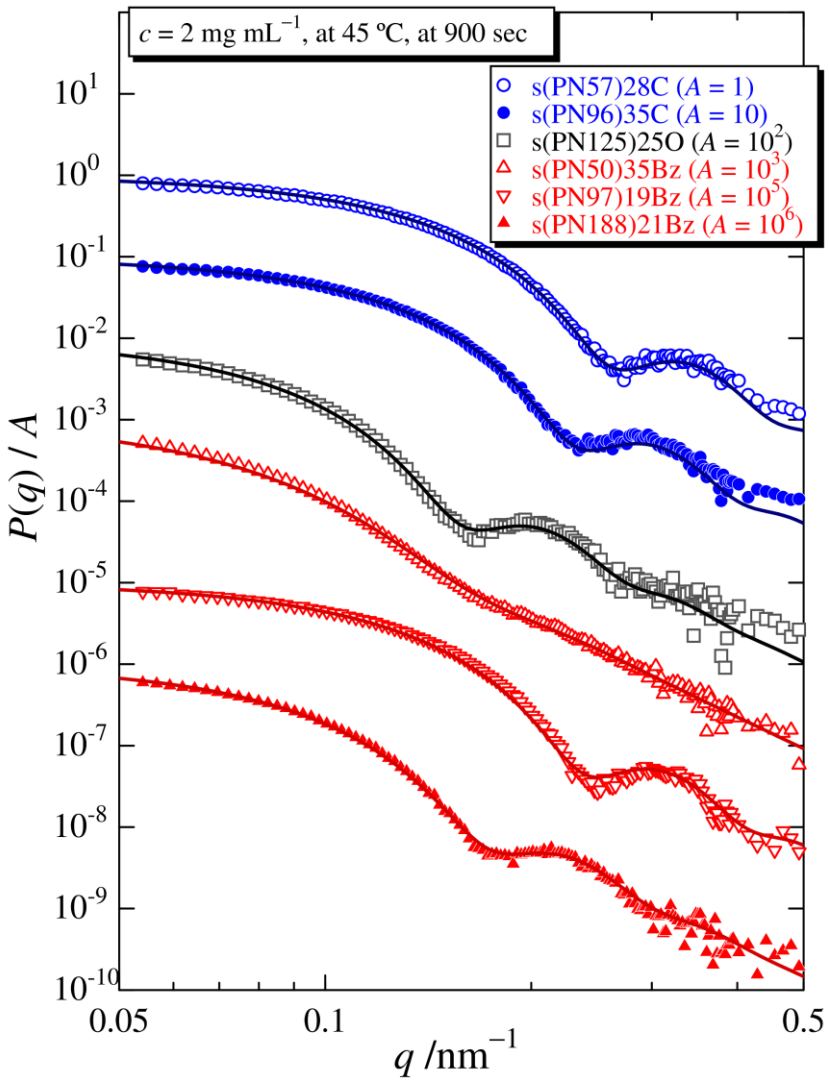

Figure 5. Double logarithmic plots of the form factor $P(q)$ vs q for the indicated sPNIPAM samples evaluated by the time-resolved SAXS experiments after rapid heating from 15 °C to 45 °C at c = 2 mg mL^{-1} and at t = 870 s. Solid curves, theoretical values for eqs 1-3 with the parameters in Table 1.

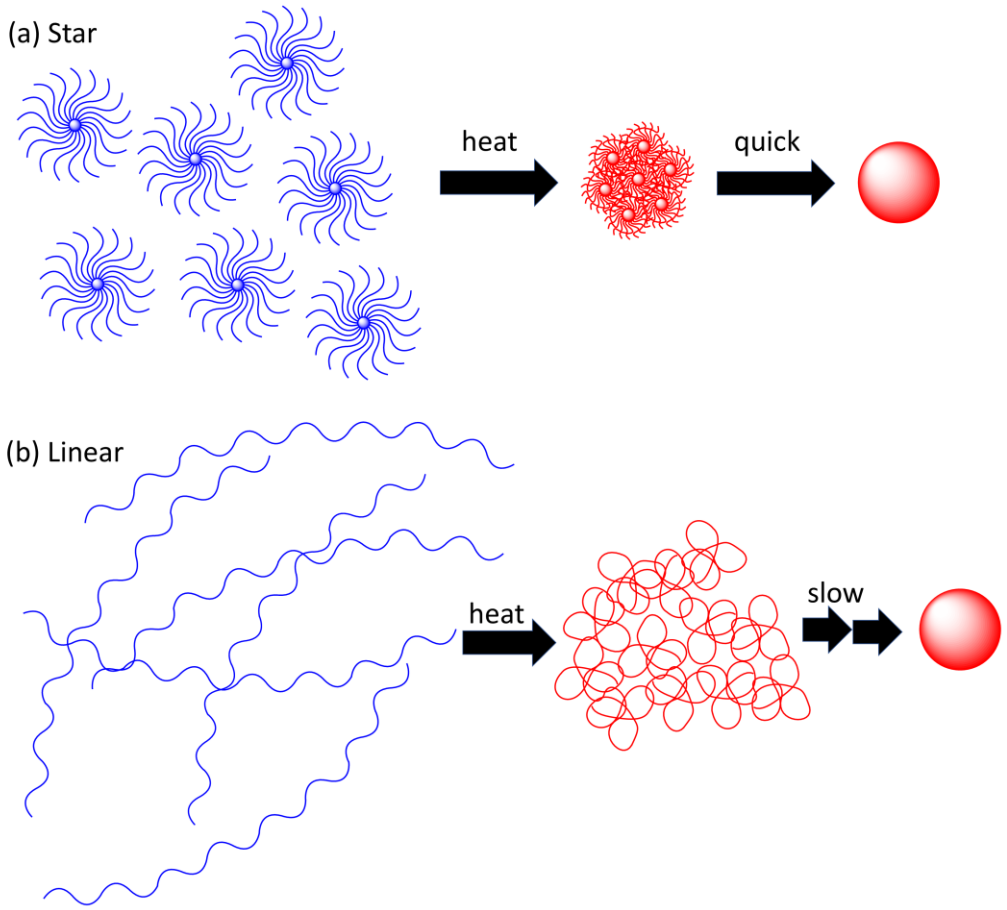

Figure 6. Schematic representation of nanodroplet formation behavior of (a) star and (b) linear PNIPAM in water.

Conclusions

Star poly(*N*-isopropylacrylamide) samples with different end groups: carboxyl, hydroxyl, and benzyl, and gel core are well soluble in water at 15 °C. The aqueous dilute solution of the samples did not become turbid even at high temperatures. Narrow-dispersed nanosized particles in water were formed with increasing temperature. Spinodal decomposition makes the narrow dispersity and the stability of the nanoparticles in water is mainly maintained by the electrostatic repulsion, which was detected by the negative ζ potential. Consequently, the dispersity index for a quickly heated solution is appreciably smaller than those for a slowly heated one. Taking into

sample-dependent size and dispersity account, they can be controlled by the arm length, arm numbers, end groups, and branching point as well as the concentration. Furthermore, the other branched polymers and linear telechelic PNIPAM with a micelle like structure[29, 30] might also be applied to obtain this phase separation-induced nanoparticle fabrication.

Supporting Information

The Supporting Information is available free of charge at http://...

Additional figures for the SAXS data for sPNIPAM samples in water and aqueous NaCl.

Notes

The authors declare no competing financial interest.

Acknowledgments

The authors are grateful to Prof. Emer. Takahiro Sato (Osaka Univ.) for fruitful discussion, Prof. Makoto Ouchi, Prof. Takaya Terashima, and Dr. Yoshihiko Kimura (Kyoto University) for performing the SEC-MALS analysis, and Dr. Noboru Ohta (SPring-8) for SAXS measurements. The synchrotron radiation experiments were performed at the BL40B2 in SPring-8 with the approval of the Japan Synchrotron Radiation Research Institute (JASRI) (proposal nos. 2019B1113, 2020A1132, 2020A0529, 2021A1092, 2021B1138, 2021B1139, 2022A1083, and 2022B1119). This work was partly supported by JSPS KAKENHI under grant numbers JP20H02788 and JP23H02011.

References

1. Halperin, A.; Kroger, M.; Winnik, F. M., Poly(N-isopropylacrylamide) Phase Diagrams: Fifty Years of Research. *Angew. Chem. Int. Ed. Engl.* **2015,** *54* (51), 15342-67.
2. Heskins, M.; Guillet, J. E., Solution Properties of Poly(N-isopropylacrylamide). *J. Macromol. Sci. A* **1968,** *2* (8), 1441-1455.
3. Kawaguchi, T.; Kobayashi, K.; Osa, M.; Yoshizaki, T., Is a "cloud-point curve" in aqueous poly(N-isopropylacrylamide) solution binodal? *J. Phys. Chem. B* **2009,** *113* (16), 5440-7.
4. Wang, X. H.; Qiu, X. P.; Wu, C., Comparison of the coil-to-globule and the globule-to-coil transitions of a single poly(N-isopropylacrylamide) homopolymer chain in water. *Macromolecules* **1998,** *31* (9), 2972-2976.
5. Gorelov, A. V.; DuChesne, A.; Dawson, K. A., Phase separation in dilute solutions of poly (N-isopropylacrylamide). *Physica A* **1997,** *240* (3-4), 443-452.
6. Aseyev, V.; Hietala, S.; Laukkanen, A.; Nuopponen, M.; Confortini, O.; Du Prez, F. E.; Tenhu, H., Mesoglobules of thermoresponsive polymers in dilute aqueous solutions above the LCST. *Polymer* **2005,** *46* (18), 7118-7131.
7. Han, J.; Takahashi, R.; Kuang, C.; Sato, T., Phase Separation Behavior of Aqueous Poly(N-isopropylacrylamide) Solutions Studied by Scattering Experiments. *Langmuir* **2022,** *38* (17), 5089-5097.
8. Kobayashi, K.; Yamada, S.; Nagaoka, K.; Kawaguchi, T.; Osa, M.; Yoshizaki, T., Characterization of Linear Poly(N-isopropylacrylamide) and Cloud Points in its Aqueous Solutions. *Polym. J.* **2009,** *41* (5), 416-424.
9. Plummer, R.; Hill, D. J. T.; Whittaker, A. K., Solution Properties of Star and Linear Poly(N-isopropylacrylamide). *Macromolecules* **2006,** *39* (24), 8379-8388.
10. Chen, Y. G.; Xiao, N.; Fukuoka, M.; Yoshida, K.; Duan, Q.; Satoh, T.; Kakuchi, T., Synthesis and thermoresponsive properties of four-arm star-shaped poly(N-isopropylacrylamide)s bearing covalent and non-covalent cores. *Polym. Chem.* **2015,** *6* (19), 3608-3616.
11. Lyngsø, J.; Al-Manasir, N.; Behrens, M. A.; Zhu, K.; Kjøniksen, A.-L.; Nyström, B.; Pedersen, J. S., Small-Angle X-ray Scattering Studies of Thermoresponsive Poly(N-isopropylacrylamide) Star Polymers in Water. *Macromolecules* **2015,** *48* (7), 2235-2243.
12. Xue, N.; Qiu, X.-P.; Chen, Y.; Satoh, T.; Kakuchi, T.; Winnik, F. M., Effect of chain architecture on the phase transition of star and cyclic poly(N-isopropylacrylamide) in water. *J. Polym. Sci., Part B: Polym. Phys.* **2016,** *54* (20), 2059-2068.
13. Luo, S.; Xu, J.; Zhu, Z.; Wu, C.; Liu, S., Phase Transition Behavior of Unimolecular Micelles with Thermoresponsive Poly(N-isopropylacrylamide) Coronas. *J. Phys. Chem. B* **2006,** *110* (18), 9132-9139.
14. Luo, S. Z.; Hu, X. L.; Zhang, Y. Y.; Ling, C. X.; Liu, X.; Chen, S. S., Synthesis of thermoresponsive unimolecular polymeric micelles with a hydrophilic hyperbranched poly(glycidol) core. *Polym. J.* **2011,** *43* (1), 41-50.
15. Ida, S.; Toyama, Y.; Takeshima, S.; Kanaoka, S., Thermoresponsive core cross-linked star-shaped poly(N-isopropylacrylamide) for reversible and controlled aggregation of nanoscale molecular units. *Polym. J.* **2020,** *52* (3), 359-363.

16. Sharker, K. K.; Takeshima, S.; Toyama, Y.; Ida, S.; Kanaoka, S.; Yusa, S.-I., pH- and thermo-responsive behavior of PNIPAM star containing terminal carboxy groups in aqueous solutions. *Polymer* **2020,** *203*, 122735.
17. Cowie, J. M. G.; Horta, A.; Mcewen, I. J.; Prochazka, K., Upper and Lower Critical Solution Temperatures for Star Branched Polystyrene in Cyclohexane. *Polym. Bull.* **1979,** *1* (5), 329-335.
18. Yokoyama, H.; Takano, A.; Okada, M.; Nose, T., Phase-Diagram of Star-Shaped Polystyrene Cyclohexane System - Location of Critical-Point and Profile of Coexistence Curve. *Polymer* **1991,** *32* (17), 3218-3224.
19. Terao, K.; Okumoto, M.; Nakamura, Y.; Norisuye, T.; Teramoto, A., Light-Scattering and Phase-Separation Studies on Cyclohexane Solutions of Four-Arm Star Polystyrene. *Macromolecules* **1998,** *31* (20), 6885-6890.
20. Tasaka, Y.; Okumoto, M.; Nakamura, Y.; Norisuye, T., Light Scattering and Phase Separation Studies on Cyclohexane Solutions of Six-Arm Star Polystyrene. *Polym. J.* **2008,** *40* (7), 634-639.
21. Shimizu, N.; Yatabe, K.; Nagatani, Y.; Saijyo, S.; Kosuge, T.; Igarashi, N., Software Development for Analysis of Small-angle X-ray Scattering Data. *AIP Conf . Proc.* **2016,** *1741* (1), 050017.
22. Tomofuji, Y.; Matsuo, K.; Terao, K., Kinetics of denaturation and renaturation processes of double-stranded helical polysaccharide, xanthan in aqueous sodium chloride. *Carbohydr. Polym.* **2022,** *275*, 118681.
23. Utashiro, Y.; Takiguchi, M.; Satoh, M., Zeta potential of PNIPAM microgel particles dispersed in water-effects of charged radical initiators vs. OH- ion adsorption. *Colloid. Polym. Sci.* **2017,** *295* (1), 45-52.
24. Van der Meeren, P.; Saveyn, H.; Bogale Kassa, S.; Doyen, W.; Leysen, R., Colloid–membrane interaction effects on flux decline during cross-flow ultrafiltration of colloidal silica on semi-ceramic membranes. *Phys. Chem. Chem. Phys.* **2004,** *6* (7), 1408-1412.
25. Shen, Z. Y.; Terao, K.; Maki, Y.; Dobashi, T.; Ma, G. H.; Yamamoto, T., Synthesis and phase behavior of aqueous poly(N-isopropylacrylamide-co-acrylamide), poly(N-isopropylacrylamide-co-N,N-dimethylacrylamide) and poly (N-isopropylacrylamide-co-2-hydroxyethyl methacrylate). *Colloid. Polym. Sci.* **2006,** *284* (9), 1001-1007.
26. Terao, K.; Otsubo, M.; Abe, M., Complex Formation of Silica Nanoparticles with Collagen: Effects of the Conformation of Collagen. *Langmuir* **2020,** *36* (47), 14425-14431.
27. Narita, T.; Yamamoto, T.; Hosoya, E.; Dobashi, T., Gibbs free energy expression for the system polystyrene in methylcyclohexane and its application to microencapsulation. *Langmuir* **2003,** *19* (13), 5240-5245.
28. Lv, W.; Liu, S.; Feng, W.; Qi, J.; Zhang, G.; Zhang, F.; Fan, X., Temperature- and Redox-Directed Multiple Self Assembly of Poly(N-Isopropylacrylamide) Grafted Dextran Nanogels. *Macromol. Rapid Commun.* **2011,** *32* (14), 1101-1107.
29. Škvarla, J.; Raya, R. K.; Uchman, M.; Zedník, J.; Procházka, K.; Garamus, V. M.; Meristoudi, A.; Pispas, S.; Štěpánek, M., Thermoresponsive behavior of poly(N-isopropylacrylamide)s with dodecyl and carboxyl terminal groups in aqueous solution: pH-dependent cloud point temperature. *Colloid. Polym. Sci.* **2017,** *295* (8), 1343-1349.
30. Lang, X. L.; Patrick, A. D.; Hammouda, B.; Hore, M. J. A., Chain terminal group leads to distinct thermoresponsive behaviors of linear PNIPAM and polymer analogs. *Polymer* **2018,** *145*, 137-147.

Supporting Information for

Temperature Induced Nanostructure Formation Behavior of Core Crosslinked Star-shaped Poly(*N*-isopropylacrylamide) in water

Ken Terao,[*,†] Masahiro Abe,[†] Masafumi Nagase,[†] Sayuri Takeshima,[‡] Shohei Ida,[‡] and Shokyoku Kanaoka[*,‡]

[†]Department of Macromolecular Science, Graduate School of Science, Osaka University, 1-1 Machikaneyama-cho, Toyonaka, Osaka 560-0043, Japan
[‡]Department of Materials Chemistry, Faculty of Engineering, The University of Shiga Prefecture, 2500 Hassaka, Hikone, Shiga 522-8533, Japan
* Corresponding author. E-mail address: terao.ken.sci@osaka-u.ac.jp

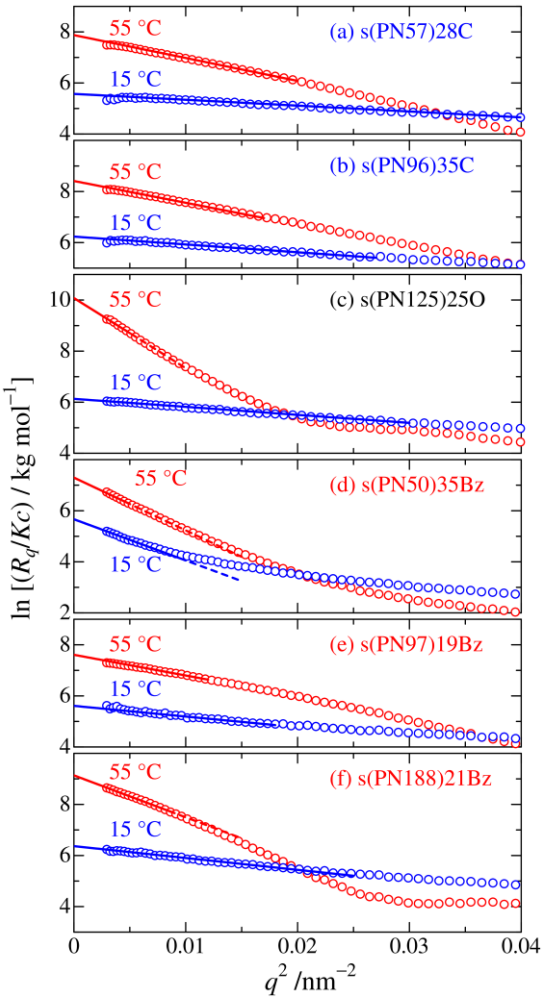

Figure S1. Guinier plots for the sPNIPAM samples in water at indicated temperatures. R_q/Kc and q are the reduced scattering intensity and the magnitude of the scattering vector, respectively. The lines indicate the initial tangent.

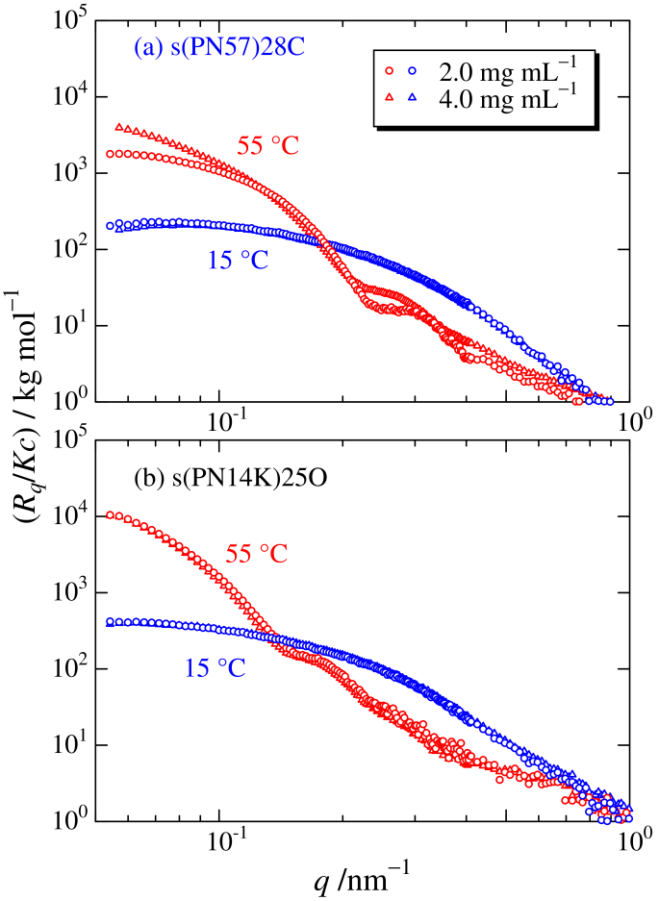

Figure S2. Double logarithmic of R_q/Kc vs q for (a) **s(PN57)28C** and (b) **s(PN14K)25O** in water at c = 2 and 4 mg mL^{-1} at indicated temperatures.

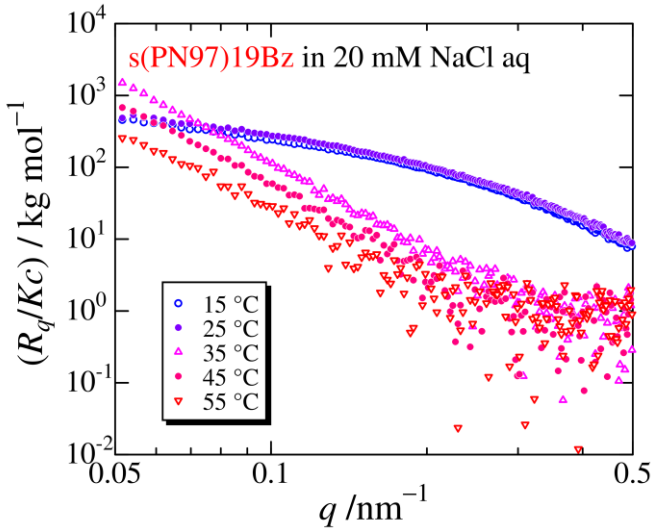

Figure S3. Double logarithmic of R_q/Kc vs q for **s(PN97)19Bz** in 20 mM aqueous NaCl at c = 2 mg mL^{-1} at indicated temperatures.

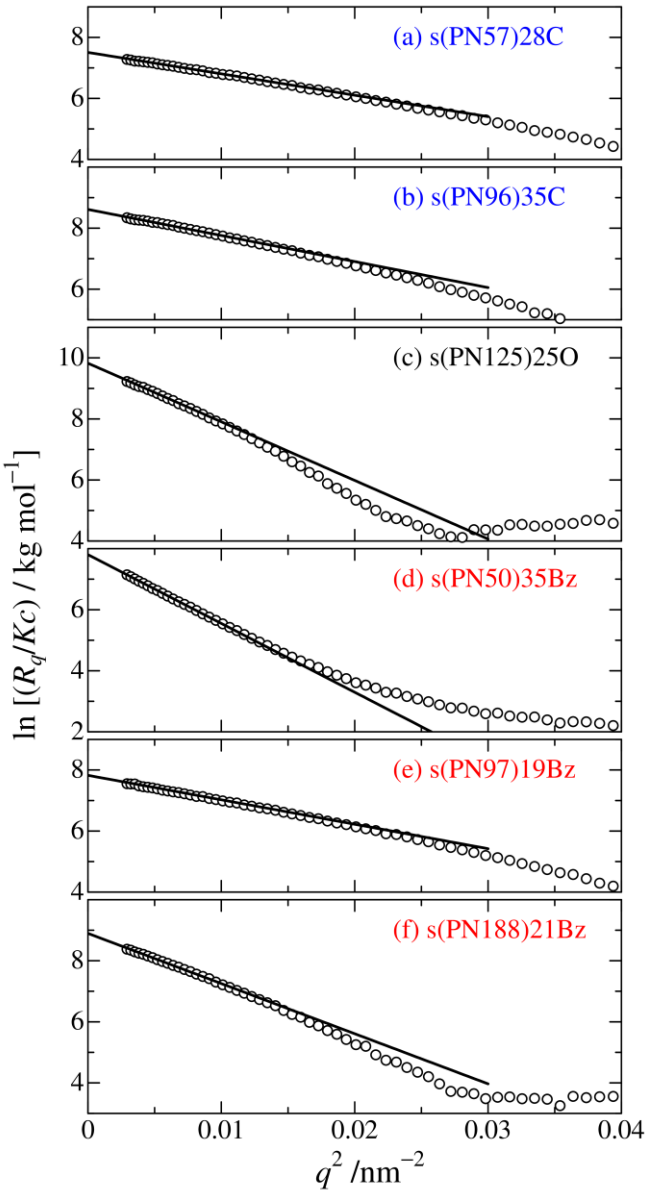

Figure S4. Guinier plots for the sPNIPAM samples in water at 45 °C temperatures after rapid heating from 15 °C and kept 900 sec.